



Published in final edited form as:

*Nat Hum Behav.* 2021 March ; 5(3): 378–388. doi:10.1038/s41562-020-00972-y.

## Distinct Regions of the Striatum Underlying Effort, Movement Initiation, and Effort Discounting

Shosuke Suzuki<sup>1</sup>, Victoria M. Lawlor<sup>1</sup>, Jessica A. Cooper<sup>1</sup>, Amanda R. Arulpragasam<sup>1</sup>, Michael T. Treadway<sup>\*,1,2</sup>

<sup>1</sup>Translational Research in Affective Disorders Laboratory, Department of Psychology, Emory University, Atlanta, GA, USA

<sup>2</sup>Department of Psychiatry and Behavioral Science, Emory University, Atlanta, GA, USA

### Abstract

The ventral striatum is believed to encode the subjective value of cost/benefit options; however, this effect has notably been absent during choices that involve physical effort. Prior work in freely-moving animals has revealed opposing striatal signals, with greater response to increasing effort demands and reduced responses to rewards requiring effort. Yet, the relationship between these conflicting signals remains unknown. Using fMRI with a naturalistic maze-navigation paradigm, we identified functionally-segregated regions within ventral striatum that separately encoded effort activation, movement initiation, and effort discounting of rewards. Additionally, activity in regions associated with effort activation and discounting oppositely predicted striatal encoding of effort during effort-based decision-making. Our results suggest that the dorsomedial region hitherto associated with action may instead represent the cost of effort, and raises fundamental questions regarding the interpretation of striatal “reward” signals in the context of effort demands. This has implications for uncovering the neural architecture underlying motivated behavior.

### Keywords

effort discounting; value-based decision-making; fMRI; naturalistic stimuli

---

Users may view, print, copy, and download text and data-mine the content in such documents, for the purposes of academic research, subject always to the full Conditions of use:[http://www.nature.com/authors/editorial\\_policies/license.html#terms](http://www.nature.com/authors/editorial_policies/license.html#terms)

\*Correspondence to: Michael T. Treadway, Department of Psychology, Emory University, Atlanta, GA 30306, p: 404-727-3166, [mtreadway@emory.edu](mailto:mtreadway@emory.edu).

#### AUTHOR CONTRIBUTIONS

SS wrote the first draft of the paper; SS and MTT designed the research; SS performed the research; SS, VML, JAC, ARA, and MTT analyzed the data; SS, VML, JAC, ARA, and MTT wrote the paper.

#### Data Availability

Contrast maps of fMRI data that support the findings of this study are available on NeuroVault (<https://neurovault.org/collections/LLQYKRMV/>). Other data are available from the corresponding author upon request.

#### Code Availability

Custom code that supports the findings of this study is available from the corresponding author upon request.

#### COMPETING INTERESTS

The authors report no conflicts of interest, financial or otherwise. In the past three years, MTT has served as a paid consultant to Blackthorn Therapeutics and Avanir Pharmaceuticals. None of these entities supported the current work, and all views expressed herein are solely those of the authors.

## Introduction

Weighing the costs and benefits of actions is critical for everyday decisions. The ventral striatum (VS) is widely recognized as a central hub for processing cost/benefit information<sup>1–3</sup>. This role for VS has been supported by robust findings from animal models implicating striatal dopamine (DA) signals in valuation and motivating movements for rewards<sup>4–8</sup>. Building upon the rich preclinical literature, human neuroimaging studies have yielded relatively homogenous results regarding the involvement of the VS in encoding subject-specific, discounted value signals<sup>1</sup>. For example, fMRI studies have demonstrated that VS responses not only are consistently greater for immediate compared to delayed rewards<sup>9–11</sup>, but also explicitly track the delay-discounted subjective value rather than the objective magnitude of rewards<sup>12–14</sup>. Similarly, VS activity is strongly associated with expected reward such that less probable rewards elicit decreased responses<sup>15,16</sup>, and tracks with the probability-discounted subjective value<sup>13</sup>. Moreover, it has been proposed that VS encodes subjective value signals that are domain-general, such that different types of cost/benefits are incorporated and represented on a common scale<sup>17</sup>. Consistent with this, VS has been shown to track subjective value regardless of whether the reward was probabilistic or delayed<sup>13</sup>. Thus, the representation of subjective value signals in the VS detected during cost/benefit decision-making has been largely consistent with the vast preclinical literature highlighting the role of striatal signaling in valuation.

A notable exception has been the neural representation of costs related to effort (i.e., the amount of work required to obtain rewards). Researchers have used various effort-based decision-making paradigms to decode effort-related value signals<sup>14,18–31</sup> with widely varying study designs (e.g., timing at which effort/reward information is presented, type and magnitude of effort demands, inclusion of effort performance during the task, inclusion of a learning component). Critically, a majority of these studies did not find a significant association between subjective value and VS activity<sup>14,19–21,23–25,27–30</sup>, not only in humans but also in rodents<sup>32</sup>. This observation is markedly at odds with prevailing theories about the functional significance of VS, and discordant with consistent patterns of value-related VS activity found in other forms of cost/benefit decision-making<sup>12–14</sup> as well as evidence demonstrating that disrupting the VS reliably impairs the willingness to work for rewards<sup>7,33,34</sup>.

Recent work examining striatal function in freely-moving animals offers one potential resolution to this discrepancy<sup>35–38</sup>. Such studies have found that DA inputs to the striatum signal the initiation of vigorous movement (“effort activation”)<sup>38</sup>, while also representing the value of cost/benefit choices that are discounted by effort-related costs (“effort discounting”)<sup>6,36</sup>. These observations raise the possibility that detection of effort-discounting signals may perhaps be hindered by the simultaneous presence of an effort-activation signal in most neuroimaging paradigms, and that critical aspects of striatal function may only be revealed by carefully parsing these opposing influences.

Importantly, these movement- and value-related signals associated with effort demands may arise from distinct neural populations within the striatum<sup>39,40</sup>. For example, prior work examining the neural substrates of goal-directed behavior has suggested that morphological

subregions of the VS, including the nucleus accumbens (NAcc) core and shell<sup>41</sup>, have different functions that together guide movements for rewards<sup>2,42</sup>. Such studies have provided evidence suggesting that neighboring regions within the VS have separable roles in processing reward- and effort-related information<sup>43–46</sup>. In a separate line of work, striatal subregions have also been identified by parcellating the striatum based on intrinsic functional connectivity<sup>47</sup>, although the functional significance of these subregions remain unclear. Notably, patterns of cortical projections to striatal subregions may play a critical role in assigning function to these subregions<sup>48</sup>. For example, inputs from reward-related areas including ventromedial prefrontal cortex (vmPFC; primarily to NAcc), orbitofrontal cortex (OFC), and dorsal anterior cingulate cortex (dACC) may converge with each other, or with inputs from regions associated with motor and cognitive functions (e.g., dorsolateral PFC; dlPFC), giving rise to striatal subregions that integrate cross-domain signals<sup>49</sup>. These reported striatal organizations raise the hypothesis that effort activation and discounting signals may originate from different subregions within VS; however, this has previously not been tested.

Additionally, the importance of including a naturalistic movement component within experimental paradigms is highlighted by evidence suggesting that (i) midbrain DA activity controls the initiation of future movement<sup>35</sup> and (ii) reward-related striatal DA inputs are attenuated in the absence of movement initiation<sup>38</sup>. To date, however, most studies investigating the mechanisms of effort-based choice in humans have focused on neural responses during the presentation or outcome of effort- or reward-related cues or choices—but not during periods of effortful movement—as the primary method with which to identify the neural substrates of subjective value<sup>14,18–31</sup>. More importantly, these prior studies have not been designed to clearly distinguish effortful or vigorous movement from mere movement. The potentially-critical role of dynamic movement raises fundamental questions regarding the interpretation of striatal “reward” signals. Notably, it has been demonstrated that naturalistic movement within virtual-reality paradigms can invoke midbrain DA neuron activity in the mouse brain<sup>50</sup>, offering a means by which this preclinical work can be translated to human neuroimaging.

Here, we combined functional magnetic resonance imaging (fMRI) with virtual navigation to evaluate activity in the human striatum associated with initiation and activation of vigorous movement (effort), initiation of simple movement (“movement”), and reward. Specifically, participants navigated through 3D mazes with the objective of obtaining rewards (Fig. 1a). Mazes varied across four conditions: Two in which individuals actively controlled navigation using (i) effortful and (ii) simple button pressing, and two in which individuals passively completed navigation (iii) with motion and (iv) without motion. To isolate the effect of effort demands on individuals’ neural responses to the anticipation and initiation of movement independently of reward expectations, reward amounts were varied independently of condition. Neural activity during the maze-navigation task was additionally examined in relation to neural responses during a second effort-based decision-making task, which was independently assessed using a paradigm previously published by our group<sup>30</sup>. During this second task, participants made choices about their willingness to perform manual button presses for monetary rewards. As such, we were able to examine neural responses to periods

of effort activation and effort discounting, and then see how they contributed to neural responses when making decisions about the value of work.

## Results

### Effort activation is represented in ventral striatal activity during anticipation and initiation of vigorous movement

To examine whether the VS encoded effort activation in the maze-navigation task, we compared hemodynamic response signals between an Effortful-Movement condition that required rapid and repeated button-pressing to move through the maze, and a Simple-Movement condition in which individuals could simply hold down buttons to move. This signal was compared at two separate timepoints: (i) when participants learned about the required effort (i.e., anticipation), and (ii) when participants began moving (i.e., initiation). Indeed, both the anticipation and initiation of Effortful- relative to Simple-Movement increased activity in a dorsal subregion of the VS extending up into dorsomedial striatum and caudate body (MNI coordinates [x, y, z] for peaks of clusters surviving whole-brain pFWE<0.05 cluster correction at two-tailed voxelwise p<0.0005, anticipation: left sub-peak: [-12, 0, 15], k=58; right sub-peak: 12, 12, 6; initiation: left sub-peak: -9, 0, 6; right sub-peak: 9, 6, -3; Fig. 1b; Supplementary Table 1). Notably, no statistically-significant effect of anticipation or initiation of movement alone was found in this effort-related dorsomedial subregion of the striatum overlapping with and extending from VS (“dmS”), evaluated by comparing the Simple-Movement condition to a Passive-Motion condition that involved automatic progression through the maze without any required finger movement. Instead, initiation of simple movements strongly recruited a distinct striatal subregion in bilateral putamen (left sub-peak: [-24, 0, -6], k=411; right sub-peak: [24, 3, -3], k=359; whole-brain pFWE<0.05 cluster-corrected at two-tailed voxelwise p<0.0005). These effects of effort activation (Effortful-Movement>Simple-Movement) and movement initiation (Simple-Movement>Passive-Motion) in dmS and putamen, respectively, were not explained by motor-related effects of button pressing (Supplementary Fig. 1). In a follow-up region-of-interest (ROI) analysis using ROIs independently-defined for each subject via leave-one-subject-out approach (see Methods; Fig. 2a–b), we found evidence for a functional dissociation between dmS (defined via Effortful-Movement>Simple-Movement contrast during initiation; Fig. 2c) and putamen (defined via Simple-Movement>Passive-Motion contrast during initiation; Fig. 2d) with respect to condition (Region\*Condition interaction:  $F_{(2,56)}=30.81$ ,  $p<0.001$ ,  $\eta^2=0.52$ , 90% confidence interval (CI): [0.35, 0.62]). Specifically, post-hoc analyses revealed evidence for a double dissociation such that dmS exhibited a disproportionate sensitivity to effort activation (Region\*Condition interaction for Effortful-Movement/Simple-Movement:  $F_{(1,28)}=6.69$ ,  $p=0.02$ ,  $\eta^2=0.19$ , 90% CI: [0.02, 0.38]; effort activation, dmS>putamen:  $t_{(28)}=2.59$ , two-tailed  $p=0.02$ ,  $d=0.48$ , 95% CI: [0.09, 0.86]) whereas putamen exhibited a disproportionate sensitivity to movement initiation (Region\*Condition interaction for Effortful-Movement/Simple-Movement:  $F_{(1,28)}=51.10$ ,  $p<0.001$ ,  $\eta^2=0.65$ , 90% CI: [0.44, 0.75]; movement initiation, putamen>dmS:  $t_{(28)}=7.15$ , two-tailed  $p<0.001$ ,  $d=1.33$ , 95% CI: [0.82, 1.82]).

### Effort discounting is represented in ventral striatal activity during reward receipt

We then examined whether VS also encoded effort discounting. Upon completion of mazes, participants were presented with a reward amount (\$0.00-\$5.00) that varied independently of the navigation condition. An anterior/ventral subregion of VS (“aVS”) responded to reward receipt (left sub-peak:  $[-3, 15, -3]$ ,  $k=27$ ; right sub-peak:  $[6, 15, -3]$ ,  $k=31$ ; whole-brain  $pFWE<0.05$  cluster-corrected at two-tailed voxelwise  $p<0.0005$ ), and was positively correlated with trial-by-trial reward magnitude (left sub-peak:  $[-6, 18, -6]$ ,  $k=65$ ; right sub-peak:  $[6, 15, -3]$ ,  $k=35$ ; whole-brain  $pFWE<0.05$  cluster-corrected at one-tailed voxelwise  $p<0.0005$ ) across all navigation conditions (Supplementary Table 1), including a No-Motion condition that involved simply waiting for the approximate duration of the maze. Importantly, while aVS exhibited a reward response within the Effortful-Movement condition ( $t_{(28)}=2.15$ , two-tailed  $p=0.04$ ,  $d=0.40$ , 95% CI:  $[0.02, 0.77]$ ), aVS response to reward was significantly lower after effortful navigation compared to navigation that required no effort ( $t_{(28)}=-1.88$ , one-tailed  $p=0.04$ ,  $d=0.35$ , 95% CI:  $[-0.03, 0.72]$ ; Fig. 2e), suggesting evidence of effort discounting. To further isolate effort discounting in the VS, we examined whether there were areas of VS that responded to reward only during the Effortful-Movement condition. This analysis isolated a region of VS that was at the intersection of aVS and dmS, suggesting a node of interaction between effort activation and effort discounting (Fig. 2f; peak:  $[6, 0, -9]$ ,  $k=72$ ; whole-brain  $pFWE<0.05$  cluster-corrected at one-tailed voxelwise  $p<0.005$ ).

### Functional segregation of effort-, movement-, and reward-related striatal subregions recapitulate connectivity-based parcellation of the striatum

Mapping together the above results (Fig. 3a), we observed functional segregation of bilateral striatal subregions associated with effort activation (dmS), reward (aVS), and simple movement (putamen). Critically, the neighboring regions associated with effort and reward showed clear evidence of double dissociation (Region\*Effect interaction:  $F_{(1,28)}=13.77$ ,  $p<0.001$ ,  $\eta^2=0.33$ , 90% CI:  $[0.10, 0.50]$ ), with dmVS responding strongly to the anticipation and initiation of effortful movement, but not receipt of reward, while aVS responded strongly to the magnitude of reward and appeared to discount reward values by effort, but showed significantly less engagement to anticipation or initiation of effortful movement ( $dmS>aVS$ , effort activation:  $t_{(28)}=2.73$ , two-tailed  $p=0.01$ ,  $d=0.51$ , 95% CI:  $[0.12, 0.89]$ ; Fig. 2c; also see Supplementary Fig. 1 for results using unsmoothed data). Notably, this functional segregation appeared to largely overlap with a previously-reported connectivity-based parcellation of the striatum<sup>47</sup> (Fig. 3a). To validate the apparent functional distinction between these two VS subregions, we compared patterns of functional connectivity during resting-state using each of the functionally-defined and connectivity-based striatal subregions as seed regions (functionally-defined seed regions: dmS: left peak:  $[-9, 0, 6]$ ; right peak:  $[9, 6, -3]$ ;  $k=264$ ; aVS: left peak:  $[-6, 18, -6]$ ; right peak:  $[6, 15, -3]$ ;  $k=77$ ; putamen: left sub-peak:  $[-24, 0, -6]$ ; right sub-peak:  $[24, 3, -3]$ ;  $k=770$ ). Indeed, despite only partial overlap of the ROI definitions derived from our task and the prior parcellation study<sup>47</sup> (Sørensen–Dice: aVS: 0.19; putamen: 0.40; dmS: 0.20), we observed highly overlapping connectivity profiles (Fig. 3b). These connectivity profiles were additionally replicated in an independent resting-state dataset collected with high-resolution (7-Tesla) fMRI<sup>51</sup> (Fig. 3b).

To further examine whether these striatal subregions participate in distinct functional networks, we evaluated direct contrasts between connectivity profiles and found notable differences in cortical regions associated with each subregion identified during maze navigation (Fig. 3c). Comparing dmS and aVS, we found that dmS has significantly stronger associations with various regions including a cluster spanning dACC and dorsomedial PFC (dmPFC; MNI peak coordinates: [-10, 20, 50],  $k=4083$ ; results are  $pFWE<0.05$  cluster-corrected at two-tailed voxelwise threshold  $p<0.005$ ), as well as a large cluster (peak: [10, 10, 8],  $k=22205$ ) including dorsolateral PFC (dlPFC), ventrolateral PFC (vlPFC), and lateral OFC, whereas aVS has significantly stronger associations with other regions including medial OFC (peak: [0, 16, -2],  $k=6040$ ) and primary motor cortex (peak: [2, -36, 60],  $k=908$ ). Comparing dmS and putamen, we found that dmS has significantly greater associations with medial PFC regions (peak: [8, 8, 0],  $k=11895$ ) and posterior cingulate cortex (PCC; peak: [6, -6, 32],  $k=1434$ ), whereas putamen has significantly greater associations with somatomotor regions (peak: [-22, 6, -2],  $k=18776$ ). Finally, comparing aVS and putamen, we found that aVS has significantly stronger associations with vmPFC and medial OFC (peak: [-14, 22, -10],  $k=6656$ ) as well as PCC (peak: [-4, -58, 14],  $k=264$ ), whereas putamen has significantly stronger associations with anterior insula and vlPFC (peak: [-24, 2, -2],  $k=10444$ ) as well as dACC and supplementary motor area (peak: [10, -6, 64],  $k=3859$ ).

### **Lack of ventral striatal activity related to value during effort-based decision-making paradigm**

To test the hypothesis that effort activation and discounting signals may interfere with the detection of subjective signals during effort-based decision-making, we also measured neural activity during a second fMRI paradigm in which participants made a series of binary choices based on the presented amount of reward and effort required for each option (Fig. 4a). Importantly, the effort and reward amounts were presented sequentially in attempt to isolate an effort-activation signal during the anticipation of various effort demands. Replicating our previous findings using this same task<sup>30</sup> as well as results from other fMRI effort-based paradigms, we did not find a statistically-significant association between VS activity and subjective value of the chosen option (whole-brain  $pFWE<0.05$  cluster-corrected with voxelwise threshold  $p<0.0005$ ; Fig. 4b; Supplementary Table 2). Even when using multivoxel pattern analysis, voxels in the VS were unable to classify whether presented information reflected reward or effort information (dmS: (mean $\pm$ s.d.) group-level accuracy=0.48 $\pm$ 0.05; aVS: (mean $\pm$ s.d.) group-level accuracy=0.48 $\pm$ 0.03; Supplementary Fig. 2). In contrast, classifiers trained on activity across all brain voxels successfully decoded whether reward or effort information was presented for 78.9% of individuals ((mean $\pm$ s.d.) group-level accuracy=0.67 $\pm$ 0.14; Supplementary Fig. 3). As described above, the absence of such an effect is noteworthy, given the robust activation of VS by subjective values derived from cost/benefit decisions involving other categories of response costs (e.g., delay, risk, or loss).

## Ventral striatal activity is modulated by opposing effects of effort activation and effort discounting

One possible explanation for the absence of effort-related subjective-value encoding in VS is that when response costs involve physical effort, opposing effort-activation and effort-discounting signals within VS may impede the ability to detect overall VS responses. To test this possibility in the maze-navigation task, we tracked responses within the VS region that responded to reward after individuals completed effortful navigation (Fig. 2f). This revealed two distinct patterns of effort-related activity in the VS depending on the timepoint, as evidenced by a significant Condition (Effortful-Movement, Simple-Movement)\*Phase (navigation initiation, reward receipt) interaction ( $F_{(1,28)}=16.72$ ,  $p=0.0003$ ,  $\eta^2=0.37$ , 90% CI: [0.14, 0.54]): VS responses were (i) significantly greater when individuals began executing effortful compared to simple movement ( $t_{(28)}=3.42$ , two-tailed  $p=0.002$ ,  $d=0.64$ , 95% CI: [0.23, 1.03]), reflecting an effort-activation signal, and (ii) significantly lower during reward receipt after individuals have expended effort compared to less effort ( $t_{(28)}=-2.66$ , two-tailed  $p=0.01$ ,  $d=0.49$ , CI: [0.10, 0.88]), reflecting an effort-discounting signal. Importantly, averaging the opposing effects associated with effort activation and effort discounting within individuals led to a statistically non-significant group-level effect ( $t_{(28)}=1.45$ , two-tailed  $p=0.16$ ,  $d=0.27$ , CI: [-0.10, 0.64]; Fig. 4c), and Bayesian analysis indicated greater preference for the hypothesis that this effect is null (Bayes factor=2.6, mean=0.08, 95% Credible Interval: [-0.04, 0.19]).

However, such “averaging” is clearly artificial, as these task conditions did not occur simultaneously. A much stronger test would therefore be to show a mix of effort activation and effort discounting signals in response to the same effort-related stimulus. We therefore extracted the “effort activation” and “effort discounting” signals from the maze-navigation task and used them as predictors of neural responses to effort cues in our second (independent) task. Interestingly, individual differences in effort-activation signal were positively associated with VS responses during presentation of effort information during decision-making ( $r_{(17)}=0.51$ ,  $p=0.02$ , 95% CI: [0.07, 0.78]), whereas individual differences in effort-discounting signals exhibited no significant correlation, but a nonsignificant trend in the opposite direction ( $r_{(17)}=-0.41$ ,  $p=0.08$ , 95% CI: [-0.73, 0.05]; Fig. 5a). These correlations were significantly different (Steiger’s  $Z=2.88$ ,  $p=0.004$ ). A post-hoc exploratory analysis using a “searchlight” approach (see Methods) revealed that opposing effects of effort activation and effort discounting signals were localized to a region at the intersection between dmS and aVS (Fig. 5b–c). Importantly, this region also encompassed 52% of the voxels within the NAcc (Fig. 5d). These findings provide a potential explanation for the longstanding discrepancy regarding the involvement of VS in encoding subjective value during effort-based decision-making epochs, as such epochs might reasonably be expected to elicit both effort-discounting and effort-activation signals.

## Discussion

For almost two decades, neural responses in the ventral striatum have been commonly observed in response to rewards and discounted value of rewards. Thus, it has been a conundrum that most functional imaging studies in humans and animals have shown weak

or inconsistent activation of VS during effort-based choice<sup>14,18–31</sup>. One methodological gap in prior studies is the failure to take into consideration striatal signals during effortful movement that have been detected under free-movement conditions in rodents<sup>35,38,52,53</sup>, which may impact the interpretation of reward-related striatal BOLD activity. Such studies have highlighted the presence of striatal signals that are heavily linked to dynamic movement<sup>35,38</sup>, which can also be evoked by movement within virtual-reality paradigms<sup>50</sup>. Thus, the present study used a virtual navigation paradigm and revealed the presence of opposite signals in the VS related to (i) effort activation during the anticipation and initiation of effortful movement and (ii) effort discounting during reward receipt after individuals expended effort. Importantly, the current study finds that effortful movement is needed to isolate these effects in the VS, as our second fMRI paradigm that relied solely on effort- and reward- cues failed to differentiate them, even when using more sensitive multivariate techniques. This observation is critical as prior studies of effort-based decision-making have largely focused on encoding of values at the point of choice or in response to feedback<sup>14,19–21,23–25,27–30</sup>. Critically, by using individual differences in estimates of effort-activation/effort-discounting signals derived from the maze navigation task, we were able to observe their simultaneous, conflicting influences when processing effort-related cues, providing a viable explanation to the general failure to detect clear subjective-value signals in the VS during effort-based decision-making in prior work. Specifically, our results suggest that increased effort requirements may invoke a greater effort-activation response that may obscure detection of the value-related effort-discounting effect in the VS, particularly within a subregion encompassing a substantial portion of NAcc.

Additionally, the current results provide insight into the functional topography of signals associated with effort, movement and reward. Despite the rich body of research implicating midbrain DA in representing value-related information and invigorating movement<sup>4</sup>, little work has been done to simultaneously examine the striatal representation of these two functions in humans. Here, we identified two striatal regions intersecting within VS—an anterior region (i.e., aVS) associated with reward and a dorsal region (i.e., dmS) associated with initiation of effortful movement—and bilateral putamen associated with initiation of simple movement. Importantly, while studies investigating neural correlates of valuation frequently report any activation, the functional localization of aVS and dmS is consistent with a prior meta-analysis<sup>1</sup> which has suggested that there may be subtle functional differences between anteroventral and dorsomedial subregions within VS. Interestingly, we observed an invigoration effect in dmS during the anticipation and initiation of effortful but not simple movement, suggesting that mere movement (i.e., making a single choice response) may not be sufficient to shape dmS signaling—further highlighting the importance of studying the neural substrates of effort-based decision-making that include effortful-movement components.

The existence of the VS subregions identified here is supported by prior large-scale connectivity results<sup>47</sup>. Indeed, we found overlap in functional-connectivity profiles between the striatal subregions identified here and the connectivity-based striatal parcellation<sup>47</sup>. Additionally, we show that each of the striatal subregions have distinct cortical connections, with dmS notably showing connectivity with dACC, OFC, and PFC regions associated with reward processing and cognitive functions, aVS showing connectivity with vmPFC and OFC



associated with reward processing, and putamen showing connectivity with sensorimotor areas. Critically, this finding helps uncover potential functions of these network-based subregions of the striatum. Our results also show similarity to the pattern of results of a recent meta-analysis of subjective-value encoding<sup>1</sup>, where positive subjective value across studies was found to scale with activity in aVS, whereas negative subjective value (i.e., loss or punishment) was associated with activity in an area similar to dmS. As activity in dmS was only apparent as a function of effort but not mere movement, whereas motor areas of putamen appeared to respond to both effortful and simple movements, it raises the intriguing possibility that dmS is more specifically involved with encoding negative value or cost associated with effortful movements. Consistent with this idea, we observed significantly greater associations with sensorimotor areas in putamen compared to dmS, further suggesting a role for dmS in processing non-motor aspects of effort. Finally, it is worth noting that similar functional heterogeneity within the ventral striatum has been observed in animal models<sup>34</sup>. Electrical recordings in non-human primates have found that distinct neuronal populations within the striatum may be responsible for coding action and outcomes<sup>39,40</sup>. In rodents, while both the NAcc core and shell are involved in Pavlovian learning of stimulus and outcome (e.g., cue and reward), they play markedly different roles in terms of mediating Pavlovian influences on instrumental behavior<sup>42,54</sup>.

There are several limitations to this study. Although the maze-navigation task was designed to parse out effects related to effort and movement, we were unable to fully isolate the two effects given that movement is an integral component of physical effort. However, given the inherent link between effort and movement, isolating the two effects may not produce ecologically-meaningful observations. Importantly, using the maze-navigation task, we were able to identify notable differences in striatal subregions associated with effort, movement, and reward, and their cortical connections that support these functions. Additionally, interpretation of the current findings are limited by the operationalization of effort employed in this study (i.e., rapid button pressing) employed in this study. Specifically, to what extent the current findings generalize to cognitive effort or other effortful tasks encountered in our daily lives remain unclear.

Taken together, our results suggest that simultaneous and conflicting influences of invigoration and value in neighboring dmS and aVS may confound the absence of subjective-value signals in effort-based decision-making tasks. It is further notable that these distinct subregions of ventral striatum were only observable when using a naturalistic paradigm, echoing recent discoveries of striatal DA function found in freely-moving animals<sup>35–38</sup>. In sum, these data will help advance our understanding of how the ventral striatum distinctly encodes effort-related costs and highlight the value of naturalistic and dynamic paradigms for achieving a deeper understanding of real-world brain function<sup>55</sup>.

## Methods

All procedures were approved by the Emory Institutional Review Board (#00077835/00101351) and informed consent was obtained from all human participants. We recruited 30 healthy adults from the Atlanta community through fliers and online advertisements. This sample size was predetermined based on previous publications<sup>28–30</sup>.

Eligibility was determined using an online pre-screening survey. Participants were eligible if they were right-handed, English-speaking individuals between the ages of 18 and 35. Exclusion criteria included: (1) MRI contraindications (e.g., claustrophobia, metallic implants, CNS diseases, pregnancy in females); (2) Current use of psychoactive medications, investigational drugs, or those that affect blood flow (e.g., for hypertension); and (3) Current medical, neurological, or psychiatric illnesses.

Participants first provided informed consent and completed the MRI safety form. Prior to MRI scanning, participants underwent a training and calibration procedure on the maze-navigation task, and on the effort-based decision-making task for a subset of the participants (n=19). In the MRI scanner, all participants completed the maze-navigation task (n=30), and two subsets of the participants completed the effort-based decision-making task (n=19) and/or a resting state scan (n=19). Participants also completed a functional localizer task designed to localize brain regions that selectively respond to visual scenes. Independent analyses using this task to examine the functional roles of scene-selective regions will be reported separately. After scanning, participants were taken to a separate interview room to complete a debriefing interview. Participants were compensated for their participation upon completion of study procedures.

Imaging data acquired from one participant during the maze-navigation task was excluded prior to analysis due to the individual falling asleep during the task. Thus, the final sample included 29 participants for the maze-navigation task analysis ( $M_{\text{age}}=24.41$ ;  $SD_{\text{age}}=5.43$ ; 21 female), 19 participants for the effort-based decision-making task ( $M_{\text{age}}=24.26$ ;  $SD_{\text{age}}=4.64$ ; 14 female), and 19 participants for the resting-state scan ( $M_{\text{age}}=24.94$ ;  $SD_{\text{age}}=5.53$ ; 12 female).

### Maze-navigation task

The task was programmed using Unity 3D (Unity Technologies ApS). A schematic of a single trial is shown in Fig. 1a. On each trial, participants completed first-person navigation through a single-path virtual maze in pursuit of monetary rewards. Each trial was associated with one of four maze structures, two of which required a single 90° turn (left or right), two of which required two 90° turns (left-then-right or right-then-left), and all of which were equated in approximate navigation time (~5s). Regardless of structure, each maze was comprised of 1×1 unit<sup>2</sup> floors placed adjacently to form a path, bounded by 1×1 unit<sup>2</sup> walls. Participants controlled movement using a 4-button box with the right (i.e., dominant) hand. Specifically, the middle finger button moved the participant forward ( $v=2.2\text{units/s}$ ), and the index and ring finger buttons each rotated the player clockwise and counterclockwise, respectively ( $\omega=0.5\pi\text{ rad/s}$ ). Holding down the buttons resulted in continuous movement or rotation (except during the Effortful-Movement condition, as detailed below). Acceleration was applied to player motion to mimic real-life motion. Only one type of motion was allowed at any given moment (i.e., pressing multiple buttons resulted in no motion). The participant view was set at 0.6 units above the floor, with a -10° tilt along the axis parallel to the ground.

Importantly, each trial was associated with one of four navigation conditions: i) The Effortful-Movement condition required participants to repeatedly press the button associated

with forward-motion to advance through the maze. In this condition, each button press moved the participant forward by an incremental distance, and the distance traveled per button press (i.e., effort level) was individually calibrated during the training procedure; ii) The Simple-Movement condition required participants to advance through the maze with the default button controls (i.e., simply hold down buttons to move and rotate). This condition served as an active-navigation control for the Effortful-Movement condition, which allows for examination of effects specifically related to vigor by subtracting out activity associated with mere movement; iii) The Passive-Motion condition required participants to view moving through the maze without making any movement. This condition served as a no-movement control for the Simple-Movement condition to examine effects related to mere movement; and iv) The No-Motion condition required participants to wait for the approximate duration of the maze (~4.7s), after which the participant was teleported to the goal. This condition served as a visual motion control for the Passive-Motion condition. Thus, two of the conditions (Effortful-Movement/Simple-Movement) required individuals to actively navigate through the maze, while the other two conditions (Passive-Motion/No-Motion) entailed passive completion of navigation. Participants failed the trial if they did not reach the goal within a liberal time-limit (5.5s) in the active navigation conditions, or if they initiated movement in the passive navigation conditions.

Each trial proceeded as follows: (1) Initial Approach phase: At the beginning of each trial, the participant position was initialized to the beginning of a maze, immediately after which participants could initiate movement. (2) Cue phase: Upon reaching a 'trigger' location in the maze, participants were rendered immobile and the floor unit immediately in view changed color for 2s, before returning to its original texture. The colored cue informed participants to the navigation condition for that trial. (3) Jittered interstimulus interval (ISI): The cue was immediately followed by a jittered fixation period, whereby a '+' was rendered on top of the maze scene for a Poisson-distributed jitter period (2–5s) with a mean duration of 2.5s. (4) Navigation phase: After the fixation cross disappeared, participants regained control of movement and completed navigation according to the navigation condition, as detailed above. On failed trials, participants were presented with a feedback screen for 2s indicating that they failed, followed by an intertrial interval (ITI; skip to (8)). (5) Jittered ISI: Upon successfully reaching the door at the end of the maze (the 'goal'), participants were again rendered immobile for another jitter period (2–5s) with a mean duration of 2.5s. (6) Reward phase: Following the ISI, participants were presented with an animation of the door opening followed by a monetary reward, represented by a dollar amount rendered on the surface of a coin. Each trial was associated with one of 4 bins of reward magnitudes (\$0, \$1.68–2.78, \$2.79–\$3.89, \$3.90–5.00), from which an amount was randomly selected. (7) Rating phase: Once every 4 trials, starting on the first trial of each run, the participant was asked to make a mood rating on a Likert-scale between 1 (not happy at all) to 4 (very happy) using button press. (8) Jittered ITI: After reward receipt, failure feedback, or mood rating, participants were presented with a '+' rendered on a grey screen for a duration (2–6s) jittered around 3s.

Prior to scanning, participants completed a 15min training procedure of the maze-navigation task. Participants were introduced to the movement controls, navigation conditions, and trial structure, and informed that a proportion of the reward they obtain on each trial will

be added to their compensation as a bonus. Once participants indicated understanding of task instructions, they completed 16 practice trials (4 per navigation condition) on a laptop computer. Participants were instructed to use the same hand and fingers that would be used to perform the task in the MRI scanner.

Each participant's average rate of key pressing during the Effortful-Movement trials were used to calibrate their effort levels for the in-scanner task. To ensure collection of button pressing rates for sufficient durations of time, the distance traveled per button press in the Effortful-Movement condition during the practice was set low (0.11 units/press) and no time-limits were imposed. However, participants were informed that there would be a time-limit for the active navigation conditions when they complete the task in the scanner and were instructed to complete the mazes during the practice as quickly as possible. From the practice data, the calibrated effort level (i.e., distance,  $d$ , per button press) for each participant was calculated as

$$d = \frac{2.2}{0.7r}$$

where  $r$  is the average key-pressing rate during the first 5.5s of the navigation phase (=time-limit on in-scanner trials) in the Effortful-Movement trials. 2.2 corresponds to the default rate of motion (unit/s). 70% of the average rate was chosen to minimize motion in the scanner, whilst maintaining similar completion times across conditions. All participants successfully completed the practice trials and demonstrated understanding of the four navigation conditions.

During the in-scanner task, the 4 navigation conditions and 4 reward bins were equally distributed and balanced across trials and runs. Each participant completed 3 runs with 32 trials each (~11min/run), and trials were presented in a fixed-randomized order. Participants successfully completed the maze on  $93 \pm 2\%$  of trials ( $M_{\text{Effortful-Movement}}=85\%$ ;  $M_{\text{Simple-Movement}}=96\%$ ,  $M_{\text{Passive-Motion}}=99\%$ ;  $M_{\text{No-Motion}}=93\%$ ), indicating low rates of failure. Importantly, mean completion times across conditions were all within 100ms ( $M_{\text{Effortful-Movement}}=4.6\text{s}$ ;  $M_{\text{Simple-Movement}}=4.5\text{s}$ ,  $M_{\text{Passive-Motion}}=4.7\text{s}$ ;  $M_{\text{No-Motion}}=4.7\text{s}$ ), suggesting that condition-based differences in "time-on-task" were unlikely to significantly affect results. Individuals initiated navigation faster on Effortful-Movement trials ( $M=550\text{ms}$ ,  $\text{s.d.}=200\text{ms}$ ) compared to Simple-Movement trials ( $M=630\text{ms}$ ,  $\text{s.d.}=210\text{ms}$ ;  $t_{(28)}=2.59$ ,  $p=0.02$ ,  $d=0.48$ ,  $\text{CI}: [0.09, 0.86]$ ). There was no evidence of a statistically-significant difference in self-reported mood ratings between the active (Effortful-/Simple-Movement;  $M=2.9$ ,  $\text{s.d.}=0.7$ ) and passive (Passive-/No-Motion) navigation conditions ( $M=2.9$ ,  $\text{s.d.}=0.7$ ;  $t_{(28)}=1.41$ ,  $p=0.17$ ,  $d=0.26$ ,  $\text{CI}: [-0.11, 0.63]$ ).

### Effort-based decision-making task

The task was previously programmed using Psychtoolbox for MATLAB<sup>30</sup>. A schematic of a single trial is shown in Fig. 4a. In this task, participants made a series of binary choices provided information about the dollar amount of the reward and the required amount of physical effort to obtain that reward for each choice option. Specifically, participants chose whether to receive \$1.00 for no work or to complete an effortful task for a larger reward of

varying amounts. On each trial, the effortful task option was associated with one of 4 bins of reward magnitude (\$1.25–2.39, \$2.40–3.49, \$3.50–4.60, and \$4.61–5.73), from which a dollar amount was randomly selected. The effort level was presented as the height of a vertical bar (20%, 50%, 80%, or 100% of the participant's individually-calibrated maximum effort level).

Prior to the scan, participants completed a training and calibration procedure. Calibration was conducted via three independent trials in which participants were asked to repeatedly press a key using their left (i.e., non-dominant) pinky finger as rapidly as possible within 20s. Each participant's maximum effort level was operationalized as the average number of keys pressed across the three trials. Participants then practiced completing the effortful tasks that varied in the required amount of key press (20, 50, 80, and 100% of their maximum effort level) within a constant time-limit (20s). They completed 4 trials at each level for a total of 16 trials. Participants were informed that the physical effort component would not be completed inside the MRI scanner, but would be completed immediately following the scan, based on the in-scanner choices. Additionally, participants were instructed that three trials would be randomly selected at the end of the session, from which the reward they earned would be added as a bonus to their compensation.

Each trial was structured as follows: Participants were first presented with either the reward or effort magnitude of the effortful option (Cue 1) on the left or right half of the screen for a jittered duration (2–6s;  $M=2.98s$ ). This information remained on the screen while the other piece of information (Cue 2) appeared on the opposite side of the screen for another jittered duration (2–6s;  $mean=3.23s$ ). Participants were then prompted to choose whether to accept the presented effortful task option, or reject the option in favor of receiving \$1.00 for no work (Choice phase). Participants indicated their choice using button press (index-finger button to accept; middle-finger button to reject), which was then presented on the screen with the words "ACCEPTED" or "REJECTED" according to their choice. Order of information (effort-then-reward vs. reward-then-effort) and the presented side of screen were counterbalanced across trials. Each participant completed 2 runs with 44 trials each (~9min/run), and trials were presented in a fixed-randomized order.

After the scan, participants were presented with each of the effortful choice options they accepted during the in-scanner task and performed the associated tasks. For each trial, participants were given the option to change their choice, to examine whether performing the effortful task in real time influenced their willingness to expend effort. We observed that choice behavior was consistent across contexts, such that participants made the same choice on  $95\pm 3\%$  of trials.

### **Behavioral and imaging data acquisition**

Stimuli were presented via back-projection mirror, and participants completed the maze-navigation and effort-choice task using an MR-compatible 4-button box (Current Designs Inc). Inflatable pads (Multipad 01; Pearltec AG) placed around participants' heads were used to minimize head motion.

Participants were scanned in a 3-Tesla Siemens TIM Trio scanner (Siemens AG) with a 32-channel head-coil using multiband structural and functional imaging<sup>56</sup>. Each session began with a 3-plane localizer scan for slice alignment, and a single-shot, high-resolution structural MPRAGE sequence (TR/TE=1900/2.27ms; flip angle=9°; FoV=250×250mm; 192×1.0mm slices). Blood oxygen level dependent functional images were acquired with T2\*-weighted EPI sequences with a multiband acceleration factor of 4 (TR/TE=1000/30.0ms; flip angle=65°; FoV=220×220mm; 52×3.00mm slices).

### Behavioral data analysis

Behavioral data from the maze-navigation task were used to examine latencies to initiate movement, rates of navigation completion, durations of navigation completion, and mood ratings. Latency to initiate movement was operationalized as the time between the offset of the jittered ISI following the Cue phase and movement onset, and was computed separately for each of the active navigation conditions (Effortful-/Simple-Movement). The rate of navigation completion was calculated as the number of successfully-completed trials divided by the total number of trials. Navigation time was calculated separately for each navigation condition, operationalized as the time between the onset of movement and reaching the goal for the active navigation trials (Effortful-/Simple-Movement), and between the offset of the jittered ISI following the Cue phase and reaching the goal for the passive navigation trials (Passive-/No-Motion). Self-reported mood ratings were averaged across trials separately across the active navigation conditions (Effortful-/Simple-Movement) and across the passive navigation conditions (Passive-/No-Motion).

Behavioral data from the effort-based decision-making task were used to compute the estimated subjective costs that individuals associate with varying levels of effort. Using custom code, participants' choice data were fit using maximum likelihood estimation to a two-parameter power function used in prior work<sup>27,30</sup>:

$$SV = R - kE^p$$

which describes subjective value (SV) as the objective reward magnitude (R) discounted by the subjective cost determined by the effort level (E; between 0–100%) that is scaled by two free parameters, k and p.

### Imaging data analysis

Functional images from the maze-navigation and effort-based decision-making tasks were preprocessed using SPM12 scripts through NeuroElf v1.1 ([neuroelf.net](http://neuroelf.net)). Specifically, images were co-registered to the structural image, motion-corrected, warped to the MNI template, and smoothed using a Gaussian filter (6mm full width-half maximum). Raw and preprocessed data were subjected to multiple tests for quality assurance and inspected for spiking and motion. Volumes were discarded if the root mean square of motion parameters exceeded a single voxel dimension (3mm), or if striping was identified through visual inspection of each functional volume. Subject-level modeling of trial events was conducted using robust regression to reduce the influence of strong outliers. Effects in group-level whole-brain analyses were considered significant at a two-tailed voxelwise

threshold of  $p < 0.0005$  combined with a cluster-extent threshold estimated for each contrast map, resulting in  $pFWE < 0.05$ , unless otherwise specified. Data distributions were assumed to be normal but this was not formally tested. For all ROI analyses, extracted parameters were entered into SPSS for significance testing and estimation of effect sizes.

For the maze-navigation task, the subject-level general linear model (GLM) included the Cue phase, first half of the Navigation phase (Navigation-Start phase), and Reward phase as regressors of interest, with each regressor separated by navigation condition. To examine the effect of reward receipt, the Reward phase was further divided into rewarded (reward  $> \$0.00$ ) and non-rewarded (reward  $= \$0.00$ ) trials. A second GLM included the trial-by-trial reward magnitude as a parametric modulator for the Reward phase, instead of separating the rewarded and non-rewarded trials. These models also included the Initial Approach phase, latter half of the Navigation phase, and Rating phase, as well as the ISIs, to omit their influences on the implicit baseline. In addition, motion parameters and their squares, as well as high-pass filter parameters were included as additional nuisance regressors. Given the potential impact of smoothing on the functional segregation of striatal subregions detected in the above models, two other GLMs were generated using unsmoothed images but otherwise following the same procedures as the first and second GLMs. Given the potential impact of button pressing on neural effects, one additional GLM was generated including each participant's number of button presses per trial as a parametric regressor for the Navigation-Start phase on Effortful- and Simple-Movement trials, but otherwise following the same procedures as the first GLM.

Group-level contrasts were generated to examine the effects of effortful movement (Effortful-Movement  $>$  Simple-Movement) and simple movement (Simple-Movement  $>$  Passive-Motion) during the Cue and Navigation Start phases, and to examine the effect of reward (Reward  $>$  No-Reward, across all conditions) and magnitude of reward (in the parametric models) during the Reward phase. One-tailed tests were used to examine regions that were positively, but not negatively, associated with reward magnitude. To examine the effect of effort on striatal response to reward, an ROI analysis was conducted by tracking responses within the aVS region found to respond to reward magnitude (left sub-peak:  $[-6, 18, -6]$ ; right sub-peak:  $[6, 15, -3]$ ;  $k=77$ ) in the parametric model. Then, we extracted beta parameters during reward receipt on rewarded trials in this independently-defined ROI, and a one-tailed pairwise comparison was conducted between the conditions that required any level of effort (Effortful-Movement/Simple-Movement) and those that did not require effort (Passive-Motion/No-Motion) to specifically examine whether reward-related aVS activity was negatively modulated by effort.

To examine the functional selectivity of striatal subregions found during the maze-navigation task, ROI analyses were conducted using a LOSO approach to avoid any circularity or non-independence in the definition of ROIs<sup>57</sup>. This was conducted by defining ROIs using group-level contrasts that include data from all but one participant; extracting beta parameters from the removed participant's data; and repeating this procedure for all participants. Beta parameters were extracted from striatal subregions associated with effortful-movement initiation (Navigation-Start phase, Effortful-Movement  $>$  Simple-Movement), simple-movement initiation (Navigation-Start

phase, Simple-Movement>Passive-Motion), and reward receipt (Reward phase, reward>no-reward, across all conditions). Effects of effortful-movement, simple-movement, and reward for each subregion was calculated by subtracting beta parameters according to the relevant contrasts (effortful-movement: Effortful-Movement – Simple-Movement; simple-movement : Simple-Movement – Passive-Motion; reward: Reward – No-Reward, averaged across navigation conditions). A 2 Region (dmS, putamen) \* 2 Effect (effortful-movement, simple-movement) repeated-measures ANOVA was conducted to test for functional dissociation between dmS and VS, and to examine whether dmS activity was selective to effortful and not mere movement. Additionally, a 2 Region (dmS, VS) \* 2 Effect (effort activation, reward receipt) repeated-measures ANOVA was conducted to test for functional dissociation between these neighboring regions associated with effort and reward.

Additionally, to examine the presence of both effort-activation and effort-discounting effects within a VS region, we functionally-defined a VS ROI (peak: [6, 0, -9]; k=72) that responded to reward after completing effortful navigation (Reward>No-Reward, Effortful-Movement condition). This reward-sensitive ROI specific to the Effortful-Movement condition was defined at a more lenient one-tailed voxelwise  $p < 0.005$  given that this region was necessarily defined on only 25% of the data. A one-tailed test was used here given our focus on identifying striatal regions increasing BOLD activity in response to reward receipt. We also note that this threshold was used for ROI definition only and not for subsequent inferential analyses. Beta parameters from this independently-defined ROI were extracted from the Effortful-Movement and Simple-Movement conditions during the Navigation Start and Reward phases, and a 2 Condition (Effortful-Movement, Simple-Movement) \* 2 Phase (Navigation Start, Reward) repeated-measures ANOVA was conducted. Pairwise comparisons were conducted to parse out the nature of significant effects. Additionally, Monte Carlo approximation (10,000 samples) was used to estimate the Bayes factor for a one-sample t-test on the average effect between the effort activation and discounting signals to examine the likelihood of a null effect. Noninformative priors were used for the mean and variance given the lack of prior work examining these opposing signals.

The CONN toolbox was used for resting-state fMRI data analysis. Preprocessing of images included motion correction, co-registration to structural scan, MNI normalization, and smoothing using an 8mm Gaussian smoothing kernel. Striatal subregions were functionally-defined from the maze-navigation data and used as seed regions to create individual seed-to-voxel functional connectivity maps. Specifically, the seed regions included a bilateral dmS region associated with effort activation (Navigation Start phase, Effortful-Movement>Simple-Movement), a region in bilateral putamen associated with movement initiation (Navigation Start phase, Simple-Movement>Passive-Motion), and a bilateral VS region associated with reward (Reward phase, parametric effect of reward magnitude, across all conditions). Two-tailed contrast maps were generated to directly compare the functional connectivity maps between each seed region in pairs (i.e., dmS>aVS, dmS>putamen, and aVS>putamen). For this analysis, we used a voxelwise height threshold of  $p < 0.005$  combined with a cluster extent threshold to achieve  $pFWE < 0.05$  given the proximity of the seed regions being compared. Additionally, for each of the three functional connectivity maps, comparison maps were generated using the spatially-corresponding subregions among



the previously-reported connectivity-based parcellation of the striatum (regions 4, 5, and 7 in the seven subregion parcellation)<sup>47</sup>. Further, functional connectivity maps using striatal regions defined from the maze-navigation task were computed using an independent set of 7T resting-state fMRI data (N=22)<sup>51</sup> downloaded from OpenNeuro ([openneuro.org](https://openneuro.org)). Specifically, two runs per subject of whole-brain resting-state data from session one in the dataset were included for the purpose of our study. Processing of these data followed the same procedures through CONN as described above, except for using a 6mm smoothing kernel to account for smaller voxel size. Lastly, Sørensen–Dice indices were calculated for each ROI defined in the maze-navigation task and the corresponding connectivity-based ROI<sup>47</sup> to test for spatial similarity between the ROI definitions. To do this, we used the nilearn—<http://nilearn.github.io>—library to resample the image space and affine of task-based ROI masks on the connectivity-based ROI masks.

For the effort-based decision-making task, the first subjective-level GLM included the Cue 1 and Cue 2 phases as regressors of interests, with Cue 1 regressors separated by type of information presented (effort vs. reward). We also included the Choice and Rating phases to omit their influence on the implicit baseline. Again, motion parameters and their squares, as well as high-pass filter parameters were included as additional nuisance regressors. At the group-level, we examined regions in which activity was higher during Cue 2 compared to Cue 1 (Cue 2>Cue 1). To examine the effect of subjective value during the valuation period, we additionally included the trial-by-trial SV of the chosen option as a parametric regressor for Cue 2 in a second GLM. At the group-level, we focused on the negative parametric effects of SV to identify regions that increased in response to decreasing value (e.g., higher effort costs). ROI analyses were conducted to examine the effect of negative SV in the dACC and VS. To do this, the dACC ROI (left sub-peak: [−10, 26, 32]; right sub-peak: [10, 24, 36]; k=334) was functionally-defined using the same parametric analysis (effect of negative SV) from our prior study using this task<sup>27,30</sup> at pFWE<0.05 cluster-corrected with one-tailed voxelwise p<0.0005, and the VS ROI was defined using an anatomical nucleus accumbens mask (left peak: [−10, 10, −8], k=309; right peak: [10, 10, −8], k=310). A one-tailed test was used to obtain results associated with the effects of negative, but not positive, SV. A pairwise comparison was conducted on the extracted parametric effects of negative SV within the dACC and VS.

Multivariate pattern analysis (MVPA) of the effort-based decision making task was performed using the scikit-learn<sup>58</sup> and nilearn libraries. We trained linear support vector machines with the C parameter fixed at a value of 1. Each classifier used unsmoothed functional images as features to predict the type of information (effort or reward) shown at Cue 1. For each trial, we selected four fMRI volumes offset by four seconds from the onset of Cue 1 presentation. Classifiers were trained and evaluated at the single-subject level using a four-fold cross validation procedure in which data were randomly partitioned into four subsets. To avoid temporal confounds, all volumes within a trial were kept in the same fold. The accuracies reported are the average of the four folds. For each subject, we tested three classifiers that differed in the spatial filtering of the images used as inputs. The first model used whole-brain images as inputs; feature selection was then performed by selecting 1,000 voxels that were most strongly associated with the training labels based on their ranking of ANOVA F-values. In the second and third models, inputs were constrained to voxels within

the aVS (left peak: [-6, 18, -6]; right peak: [6, 15, -3]; k=77) and dmS (left peak: [-9, 0, 6]; right peak: [9, 6, -3]; k=264) masks, respectively. To test the significance of classifier performance, we ran permutation tests in which the same classification procedure was repeated using 1,000 random permutations of training labels<sup>59</sup>. This provided a distribution of chance-level accuracy; we consider the performance of a classifier as significantly above chance if is greater than 95% of accuracies obtained using permuted tests<sup>59</sup>.

Additionally, to examine whether individual differences in striatal responses during maze-navigation predicted ventral striatal signals in the effort-based decision-making task, we used the extracted beta parameters from the dmS (obtained from Navigation Start phase, Effortful-Movement>Simple-Movement; left peak: [-9, 0, 6]; right peak: [9, 6, -3]; k=264) and VS (obtained from Reward phase, Reward>No-Reward, Effortful-Movement condition; peak: [6, 0, -9]; k=72) to compute individual differences in the effect of effort (Effortful-Movement – Simple-Movement) during the Navigation-Start phase for dmS (i.e., effort activation signal) and during the Reward phase for VS (i.e., effort discounting signal). We then correlated these effects with extracted beta parameters from the VS during an open contrast of the presentation of effort information at Cue 1 (averaged across all presented effort levels) in the effort-based decision-making task. An open contrast (i.e., contrasted against the implicit baseline) was used as we felt this best represented neural responses to potential effort as compared to the default “no effort” option that was always available to participants on this task. Further, to localize locations within the striatum where effort activation and discounting signals had significant opposing effects, a post-hoc exploratory analysis was conducted using NeuroElf and custom code. For each voxel within a striatal mask<sup>47</sup> (k=37,551), we defined a spherical ROI (r=2mm) and removed any voxels residing outside of the mask. Then, we extracted parameters from each of these ROIs during the presentation of effort information in the effort-based decision-making task, and correlated these parameters with the effort activation and discounting signals from the maze-navigation task. Steiger’s Z test was used to compare correlation coefficients across these analyses. Voxels in which there were significant differences in correlation coefficients were compared with voxels in bilateral NAcc as defined in the Harvard-Oxford atlas distributed with FSL (<http://www.fmrib.ox.ac.uk/fsl/>).

## Supplementary Material

Refer to Web version on PubMed Central for supplementary material.

## ACKNOWLEDGEMENTS

This work was supported by funding from the NIMH R00 MH102355 and R01 MH108605 to MTT and F32 MH115692 to JAC, and the National Science Foundation Graduate Research Fellowship Program DGE- 1444932 to ARA. The funders had no role in study design, data collection and analysis, decision to publish or preparation of the manuscript. The authors would like to thank Joshua Buckholtz and Daniel Dilks for helpful discussion and commentary. The authors additionally thank Brittany DeVries, Makiah Nuutinen, Emma Hahn, Danielle Harrison, Annabel Lu, Maryam Rehman, Jeffrey Yang, Kristi Kwok, Samuel Han, and Nimra Ahad for their assistance in data collection.

## References

1. Bartra O, McGuire JT & Kable JW The valuation system: a coordinate-based meta-analysis of BOLD fMRI experiments examining neural correlates of subjective value. *Neuroimage* 76, 412–427 (2013). [PubMed: 23507394]
2. Mogenson GJ, Jones DL & Yim CY From motivation to action: functional interface between the limbic system and the motor system. *Progress in Neurobiology* 14, 69–97 (1980). [PubMed: 6999537]
3. Knutson B, Delgado MR & Phillips PE in *Neuroeconomics: Decision Making and the Brain* 389–406 (Academic Press, 2009).
4. Berke JD What does dopamine mean? *Nature Neuroscience* 21, 787–793 (2018). [PubMed: 29760524]
5. Berridge KC & Robinson TE What is the role of dopamine in reward: hedonic impact, reward learning, or incentive salience? *Brain Research Reviews* 28, 309–369 (1998). [PubMed: 9858756]
6. Schultz W, Carelli RM & Wightman RM Phasic dopamine signals: from subjective reward value to formal economic utility. *Current Opinion in Behavioral Sciences* 5, 147–154 (2015). [PubMed: 26719853]
7. Salamone JD, Correa M, Farrar A & Mingote SM Effort-related functions of nucleus accumbens dopamine and associated forebrain circuits. *Psychopharmacology* 191, 461–482 (2007). [PubMed: 17225164]
8. Wise RA Dopamine, learning and motivation. *Nature Reviews Neuroscience* 5, 483 (2004). [PubMed: 15152198]
9. McClure SM, Laibson DI, Loewenstein G & Cohen JD Separate neural systems value immediate and delayed monetary rewards. *Science* 306, 503–507 (2004). [PubMed: 15486304]
10. Wittmann M, Leland DS & Paulus MP Time and decision making: differential contribution of the posterior insular cortex and the striatum during a delay discounting task. *Experimental Brain Research* 179, 643–653 (2007). [PubMed: 17216152]
11. Gregorios-Pippas L, Tobler PN & Schultz W Short term temporal discounting of reward value in human ventral striatum. *Journal of Neurophysiology* 101, 1507–1523 (2009). [PubMed: 19164109]
12. Kable JW & Glimcher PW The neural correlates of subjective value during intertemporal choice. *Nature Neuroscience* 10, 1625 (2007). [PubMed: 17982449]
13. Peters J & Büchel C Overlapping and distinct neural systems code for subjective value during intertemporal and risky decision making. *Journal of Neuroscience* 29, 15727–15734 (2009). [PubMed: 20016088]
14. Prévost C, Pessiglione M, Météreau E, Cléry-Melin M-L & Dreher J-C Separate valuation subsystems for delay and effort decision costs. *Journal of Neuroscience* 30, 14080–14090 (2010). [PubMed: 20962229]
15. Abler B, Walter H, Erk S, Kammerer H & Spitzer M Prediction error as a linear function of reward probability is coded in human nucleus accumbens. *Neuroimage* 31, 790–795 (2006). [PubMed: 16487726]
16. Yacubian J et al. Dissociable systems for gain-and loss-related value predictions and errors of prediction in the human brain. *Journal of Neuroscience* 26, 9530–9537 (2006). [PubMed: 16971537]
17. Levy DJ & Glimcher PW The root of all value: a neural common currency for choice. *Current Opinion in Neurobiology* 22, 1027–1038 (2012). [PubMed: 22766486]
18. Croxson PL, Walton ME, O'Reilly JX, Behrens TE & Rushworth MF Effort-based cost–benefit valuation and the human brain. *Journal of Neuroscience* 29, 4531–4541 (2009). [PubMed: 19357278]
19. Kurniawan IT et al. Choosing to make an effort: the role of striatum in signaling physical effort of a chosen action. *Journal of Neurophysiology* 104, 313–321 (2010). [PubMed: 20463204]
20. Schmidt L, Lebreton M, Cléry-Melin M-L, Daunizeau J & Pessiglione M Neural mechanisms underlying motivation of mental versus physical effort. *PLoS Biology* 10, e1001266 (2012). [PubMed: 22363208]

21. Burke CJ, Brünger C, Kahnt T, Park SQ & Tobler PN Neural integration of risk and effort costs by the frontal pole: only upon request. *Journal of Neuroscience* 33, 1706–1713 (2013). [PubMed: 23345243]
22. Kurniawan IT, Guitart-Masip M, Dayan P & Dolan RJ Effort and valuation in the brain: the effects of anticipation and execution. *Journal of Neuroscience* 33, 6160–6169 (2013). [PubMed: 23554497]
23. Skvortsova V, Palminteri S & Pessiglione M Learning to minimize efforts versus maximizing rewards: computational principles and neural correlates. *Journal of Neuroscience* 34, 15621–15630 (2014). [PubMed: 25411490]
24. Massar SA, Libedinsky C, Weiyan C, Huettel SA & Chee MW Separate and overlapping brain areas encode subjective value during delay and effort discounting. *NeuroImage* 120, 104–113 (2015). [PubMed: 26163803]
25. Scholl J et al. The good, the bad, and the irrelevant: neural mechanisms of learning real and hypothetical rewards and effort. *Journal of Neuroscience* 35, 11233–11251 (2015). [PubMed: 26269633]
26. Bonnelle V, Manohar S, Behrens T & Husain M Individual differences in premotor brain systems underlie behavioral apathy. *Cerebral Cortex* 26, 807–819 (2015). [PubMed: 26564255]
27. Klein-Flügge MC, Kennerley SW, Saraiva AC, Penny WD & Bestmann S Behavioral modeling of human choices reveals dissociable effects of physical effort and temporal delay on reward devaluation. *PLoS Computational Biology* 11, e1004116 (2015). [PubMed: 25816114]
28. Chong TT-J et al. Neurocomputational mechanisms underlying subjective valuation of effort costs. *PLoS Biology* 15, e1002598 (2017). [PubMed: 28234892]
29. Hauser TU, Eldar E & Dolan RJ Separate mesocortical and mesolimbic pathways encode effort and reward learning signals. *Proceedings of the National Academy of Sciences* 114, E7395–E7404 (2017).
30. Arulpragasam AR, Cooper JA, Nuutinen MR & Treadway MT Corticoinsular circuits encode subjective value expectation and violation for effortful goal-directed behavior. *Proceedings of the National Academy of Sciences* 115, E5233–E5242 (2018).
31. Aridan N, Malecek NJ, Poldrack RA & Schonberg T Neural correlates of effort-based valuation with prospective choices. *NeuroImage* 185, 446–454 (2019). [PubMed: 30347281]
32. Endepols H et al. Effort-based decision making in the rat: an [18F] fluorodeoxyglucose micro positron emission tomography study. *Journal of Neuroscience* 30, 9708–9714 (2010). [PubMed: 20660253]
33. Cousins MS & Salamone JD Nucleus accumbens dopamine depletions in rats affect relative response allocation in a novel cost/benefit procedure. *Pharmacology Biochemistry and Behavior* 49, 85–91 (1994).
34. Floresco SB The nucleus accumbens: an interface between cognition, emotion, and action. *Annual Review of Psychology* 66, 25–52 (2015).
35. da Silva JA, Tecuapetla F, Paixão V & Costa RM Dopamine neuron activity before action initiation gates and invigorates future movements. *Nature* 554, 244 (2018). [PubMed: 29420469]
36. Day JJ, Jones JL, Wightman RM & Carelli RM Phasic nucleus accumbens dopamine release encodes effort-and delay-related costs. *Biological Psychiatry* 68, 306–309 (2010). [PubMed: 20452572]
37. Hamid AA et al. Mesolimbic dopamine signals the value of work. *Nature neuroscience* 19, 117 (2016). [PubMed: 26595651]
38. Syed EC et al. Action initiation shapes mesolimbic dopamine encoding of future rewards. *Nature Neuroscience* 19, 34–39 (2016). [PubMed: 26642087]
39. Lau B & Glimcher PW Action and outcome encoding in the primate caudate nucleus. *Journal of Neuroscience* 27, 14502–14514 (2007). [PubMed: 18160658]
40. Samejima K, Ueda Y, Doya K & Kimura M Representation of action-specific reward values in the striatum. *Science* 310, 1337–1340 (2005). [PubMed: 16311337]
41. Zaborszky L et al. Cholecystokinin innervation of the ventral striatum: a morphological and radioimmunological study. *Neuroscience* 14, 427–453 (1985). [PubMed: 3887206]

42. Penner MR & Mizumori SJ Neural systems analysis of decision making during goal-directed navigation. *Progress in Neurobiology* 96, 96–135 (2012). [PubMed: 21964237]
43. Di Chiara G et al. Dopamine and drug addiction: the nucleus accumbens shell connection. *Neuropharmacology* 47, 227–241 (2004). [PubMed: 15464140]
44. Van Der Plasse G, Schrama R, Van Seters SP, Vanderschuren LJ & Westenberg HG Deep brain stimulation reveals a dissociation of consummatory and motivated behaviour in the medial and lateral nucleus accumbens shell of the rat. *PloS One* 7, e33455 (2012). [PubMed: 22428054]
45. Parkinson JA, Willoughby PJ, Robbins TW & Everitt BJ Disconnection of the anterior cingulate cortex and nucleus accumbens core impairs Pavlovian approach behavior: Further evidence for limbic cortical–ventral striatopallidal systems. *Behavioral Neuroscience* 114, 42 (2000). [PubMed: 10718261]
46. Ko D & Wanat MJ Phasic dopamine transmission reflects initiation vigor and exerted effort in an action-and region-specific manner. *Journal of Neuroscience* 36, 2202–2211 (2016). [PubMed: 26888930]
47. Choi EY, Yeo BT & Buckner RL The organization of the human striatum estimated by intrinsic functional connectivity. *Journal of Neurophysiology* 108, 2242–2263 (2012). [PubMed: 22832566]
48. Haber SN & Knutson B The reward circuit: linking primate anatomy and human imaging. *Neuropsychopharmacology* 35, 4–26 (2010). [PubMed: 19812543]
49. Haber SN, Kim K-S, Maily P & Calzavara R Reward-related cortical inputs define a large striatal region in primates that interface with associative cortical connections, providing a substrate for incentive-based learning. *Journal of Neuroscience* 26, 8368–8376 (2006). [PubMed: 16899732]
50. Engelhard B et al. Specialized coding of sensory, motor and cognitive variables in VTA dopamine neurons. *Nature*, 570, 509–513 (2019). [PubMed: 31142844]
51. Gorgolewski KJ et al. A high resolution 7-Tesla resting-state fMRI test-retest dataset with cognitive and physiological measures. *Scientific Data* 2, 140054 (2015). [PubMed: 25977805]
52. Howe MW, Tierney PL, Sandberg SG, Phillips PE & Graybiel AM Prolonged dopamine signalling in striatum signals proximity and value of distant rewards. *Nature* 500, 575–579 (2013). [PubMed: 23913271]
53. Roesch MR, Singh T, Brown PL, Mullins SE & Schoenbaum G Ventral striatal neurons encode the value of the chosen action in rats deciding between differently delayed or sized rewards. *Journal of Neuroscience* 29, 13365–13376 (2009). [PubMed: 19846724]
54. Hall J, Parkinson JA, Connor TM, Dickinson A & Everitt BJ Involvement of the central nucleus of the amygdala and nucleus accumbens core in mediating Pavlovian influences on instrumental behaviour. *European Journal of Neuroscience* 13, 1984–1992 (2001).
55. Sonkusare S, Breakspear M & Guo C Naturalistic Stimuli in Neuroscience: Critically Acclaimed. *Trends in Cognitive Sciences* 23, 699–714 (2019). [PubMed: 31257145]
56. Van Essen DC et al. The WU-Minn human connectome project: an overview. *Neuroimage* 80, 62–79 (2013). [PubMed: 23684880]
57. Esterman M, Tamber-Rosenau BJ, Chiu Y-C & Yantis S Avoiding non-independence in fMRI data analysis: leave one subject out. *Neuroimage* 50, 572–576 (2010). [PubMed: 20006712]
58. Pedregosa F et al. Scikit-learn: Machine learning in Python. *Journal of Machine Learning Research* 12, 2825–2830 (2011).
59. Ojala M & Garriga GC Permutation tests for studying classifier performance. *Journal of Machine Learning Research* 11, 1833–1863 (2010).

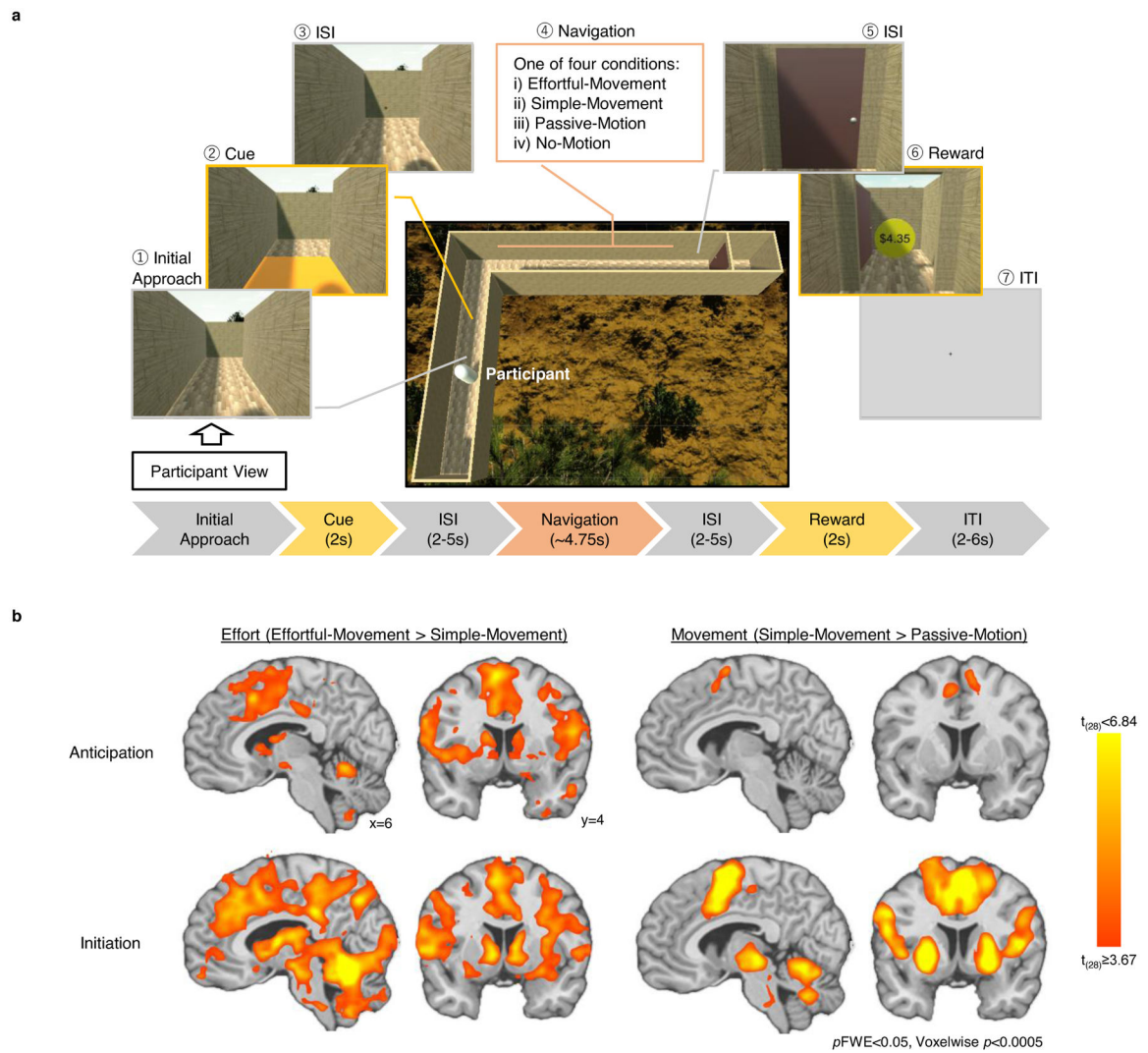


**Fig. 1. Maze-navigation task schematic and whole-brain results (N=29).**

(a) Schematic of a task trial. (b) Whole-brain results examining the effect of effortful and simple movement during anticipation and initiation of navigation. Maps are  $p < 0.05$  familywise-error (pFWE) cluster-corrected with voxelwise threshold  $p < 0.0005$ .

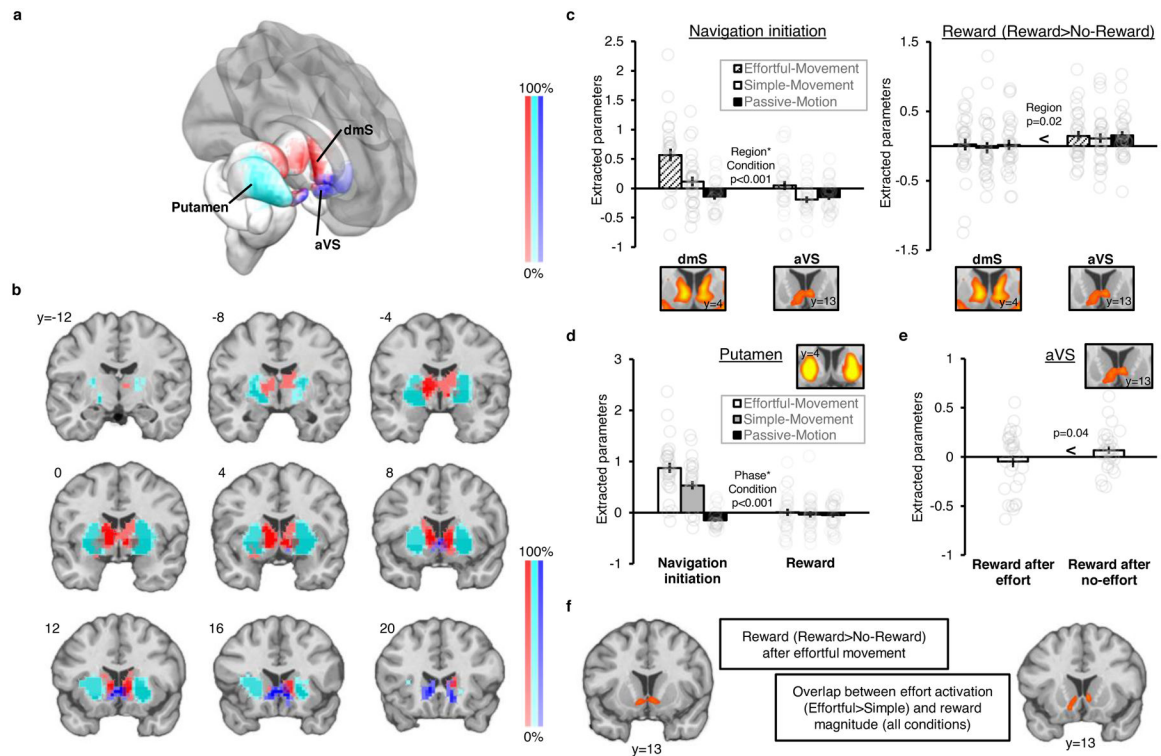


**Fig. 2. Maze-navigation task ROI analyses and results (N=29).**

Degree of overlap between ROIs defined for each participant using the leave-one-subject-out approach, including dmS (depicted in red), aVS (depicted in blue), and putamen (depicted in light blue), mapped on (a) a subcortical surface and (b) coronal sections ( $y=-12$  to  $20$ ). ROIs were defined using  $pFWE < 0.05$  cluster correction with voxelwise threshold  $p < 0.0005$ . (c) dmS and aVS response to navigation initiation and reward. A significant Region\*Effect (effort activation, reward receipt) interaction ( $F_{(1,28)}=13.77$ ,  $p < 0.001$ ,  $\eta^2=0.33$ , 90% CI: [0.10, 0.50]) suggests functional dissociation between dmS and aVS. (d) Putamen response to navigation initiation and reward. (e) Reward response in aVS is significantly reduced after any level of effort (Effortful-Movement/Simple-Movement) compared to non-effortful conditions (Passive-Motion/No-Motion);  $t_{(28)}=-1.88$ , one-tailed  $p=0.04$ ,  $d=0.35$ , 95% CI: [-0.03, 0.72]). (f) VS response to reward after effortful navigation and conjunction between effects of effort activation (Effortful-Movement>Simple-Movement, navigation initiation) and reward magnitude (across all conditions, reward phase). Maps are  $pFWE < 0.05$  cluster-corrected with voxelwise threshold  $p < 0.0005$ . Error bars in bar plots represent standard error of the mean.

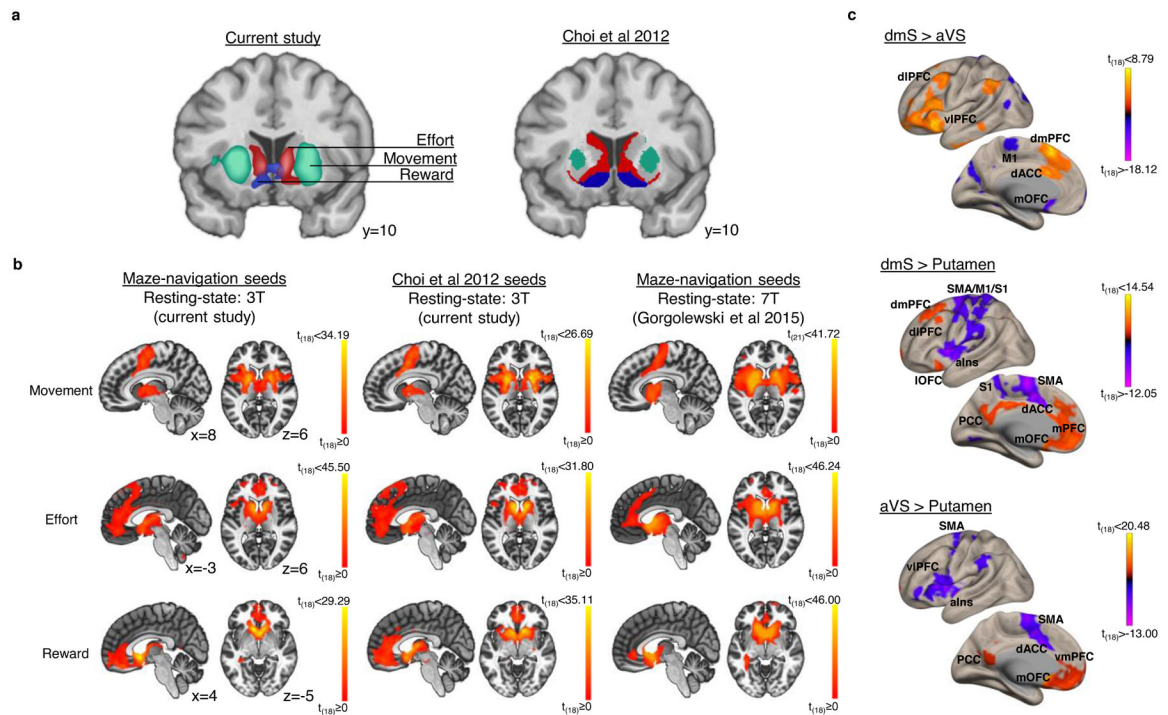


**Fig. 3. Functional segregation of striatum and comparison of connectivity profiles with previously-identified striatal parcellation based on intrinsic connectivity.**

(a) Striatal subregions identified in the current study ( $N=29$ ) and corresponding subregions identified via connectivity-based parcellation<sup>47</sup>. (b) Seed-to-voxel functional connectivity maps using striatal regions in (a) as seed regions and resting-state data from the current study ( $N=19$ ) and prior work ( $N=22$ )<sup>51</sup>. Maps are pFWE $<0.05$  cluster-corrected with voxelwise threshold  $p<0.0005$ . (c) Comparisons between functional connectivity maps using different striatal seed regions ( $N=19$ ). Maps are pFWE $<0.05$  cluster-corrected with voxelwise threshold  $p<0.005$ . The contrast label indicates the seed regions being compared. A lateral and medial view of the left hemisphere is shown for each contrast. aIns: anterior insula; vIPFC: ventrolateral prefrontal cortex; dmPFC: dorsomedial prefrontal cortex; IOFC: lateral orbital frontal cortex; mOFC: medial orbital frontal cortex; M1: primary motor cortex; S1: somatosensory cortex; SMA: supplementary motor area; PCC: posterior cingulate cortex.



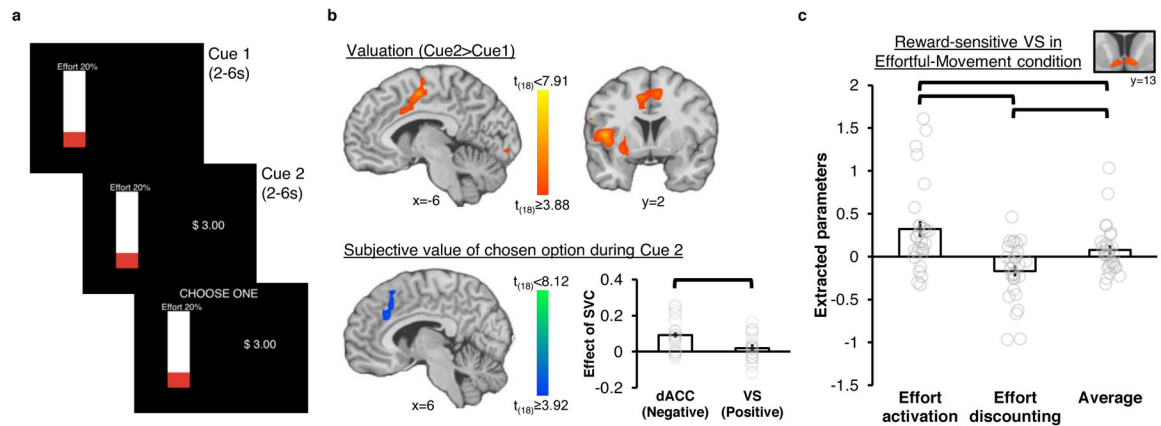


**Fig. 4. Schematic and results of effort-based decision-making (EBDM) task (N=19).**

(a) Schematic of a task trial. (b) Whole-brain results replicate our prior findings using this paradigm<sup>30</sup>, including activation of dorsal anterior cingulate cortex (dACC) and insula at Cue 2, association between dACC and negative subjective value, and lack of statistically-significant evidence of VS response across contrasts (difference:  $t_{(18)}=2.15$ ,  $p=0.05$ ,  $d=0.49$ , 95% CI: [0.01, 0.96]). Maps are pFWE<0.05 cluster-corrected with voxelwise threshold  $p<0.0005$ . (c) aVS encodes both effort activation (Effortful-Movement>Simple-Movement at navigation initiation;  $t_{(28)}=3.42$ ,  $p=0.002$ ,  $d=0.64$ , 95% CI: [0.23, 1.03]) and effort discounting (Effortful-Movement>Simple-Movement at reward receipt;  $t_{(28)}=-2.66$ ,  $p=0.01$ ,  $d=0.49$ , 95% CI: [0.10, 0.88]) that average to a statistically non-significant group effect ( $t_{(28)}=1.45$ , two-tailed  $p=0.16$ ,  $d=0.27$ , CI: [-0.10, 0.64]). Error bars in bar plots represent standard error of the mean.

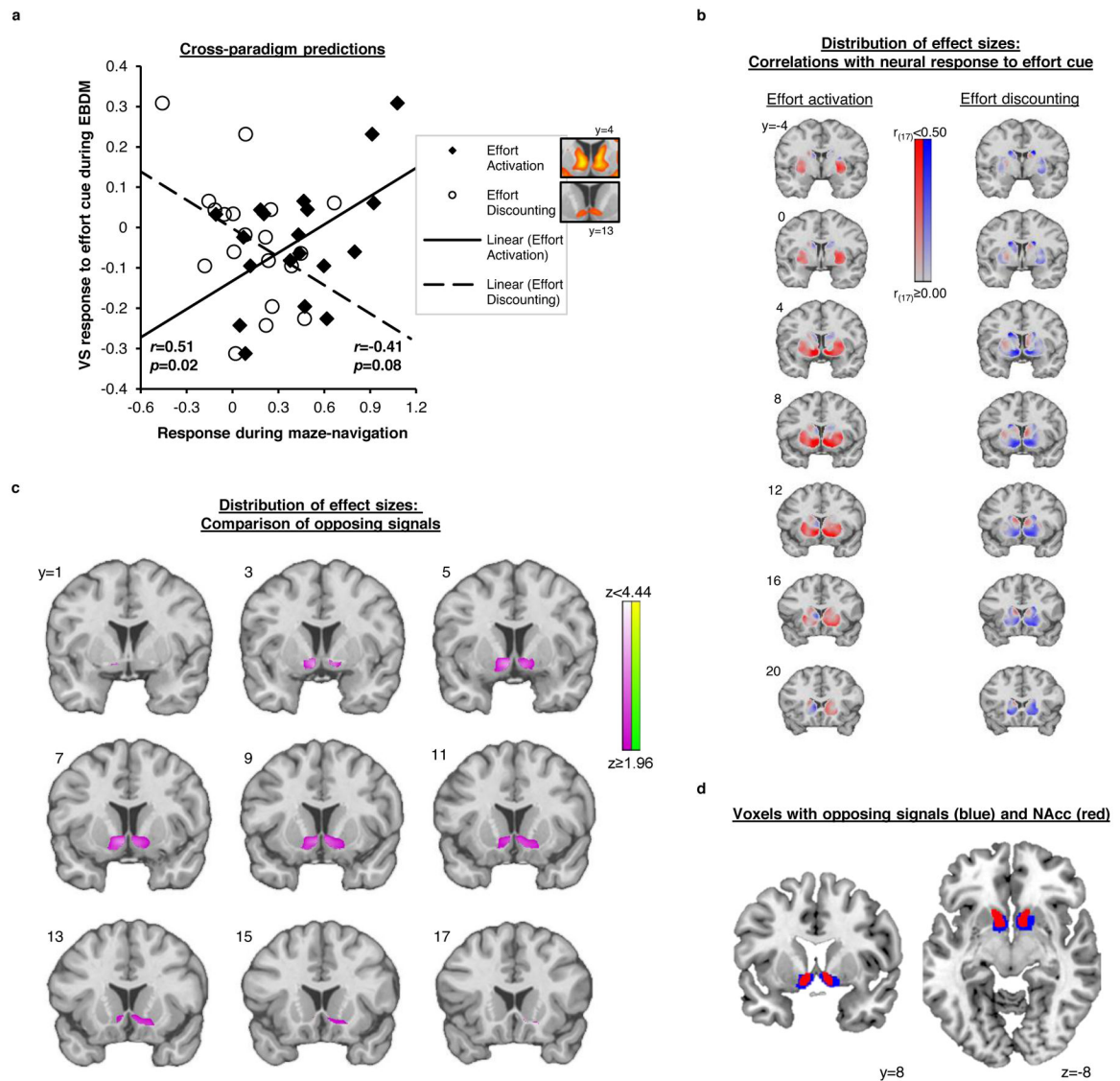


**Fig. 5. Cross-paradigm analyses (N=19).**

(a) Effort activation and discounting signals during maze-navigation are oppositely associated with VS responses to effort information during EBDM (effort activation:  $r(17)=0.51$ ,  $p=0.02$ , 95% CI: [0.07, 0.78]; effort discounting:  $r(17)=-0.41$ ,  $p=0.08$ , 95% CI: [-0.73, 0.05]; Steiger's  $Z=2.88$ ,  $p=0.004$ ). X-axis represents magnitude of effort activation and discounting responses in respective striatal subregions during maze navigation. (b) Distribution of effects sizes for correlations between neural response to effort information with effort activation and discounting signals within spherical ROIs defined at each striatal voxel. (c) Voxels in which correlation coefficients in (b) were found to be significantly different. (d) Comparison of voxels with opposing effort activation and discounting signals (in blue) and NAcc (in red). 52% of NAcc voxels are encompassed in the region showing opposing signals.